

## Relationship Between Particle Size and Dissolution Rate of Bulk Powders and Sieving Characterized Fractions of Two Qualities of Orthoboric Acid

A. Tromelin, S. Habillon, C. Andrès, Y. Pourcelot, and B. Chaillot

Groupe Physico-Chimie et Technologie des Poudres Pharmaceutiques,  
Université de Bourgogne, Faculté de Pharmacie, 7 boulevard Jeanne  
d'Arc, 21033 Dijon, France

### ABSTRACT

*We have carried out a study of the particle size distribution and aqueous dissolution rate of two commercially available qualities of orthoboric acid, labeled "crystal" (ABC) and "powder" (ABP). In a previous work, we have shown that the two commercial qualities of orthoboric acid chosen as model compound ("powder" and "crystal") are related to the same crystal network in spite of their different names. However, these two qualities have very different size particle distributions, as previously determined by sieving and confirmed by the present laser light scattering study. Dissolution testing is performed under sink conditions and show that the bulk ABC quality dissolves far more rapidly than the bulk ABP quality. For each quality, dissolution rates of four sieved particle size fractions (0–90  $\mu\text{m}$ ; 90–125  $\mu\text{m}$ ; 125–180  $\mu\text{m}$ ; 180–250  $\mu\text{m}$ ) were compared. Concerning the ABC quality, comparisons were also done with three other particles size fractions: 250–355  $\mu\text{m}$ , 355–500  $\mu\text{m}$ , and 500–710  $\mu\text{m}$ . This study used the  $dQ/dt$  versus  $t$  profile. Dissolution profiles of the fractions enclosing particles with a size superior to 125  $\mu\text{m}$  are very close. On the other hand, fractions enclosing particles with a size smaller than 90  $\mu\text{m}$  present a different profile and a slower rate of dissolution.*

## INTRODUCTION

The rate of dissolution of a drug in aqueous media is often the rate-limiting step in its systemic bioavailability. Pharmaceutical powder is a granular medium and it is widely known that several factors such as surface morphology, degree of porosity, surface area, particle shape, and particle size of a drug have significant effects on its physicochemical properties in relation to the dissolution rate.

Particle size distribution and particle shape effect on dissolution performance have been the subject of several publications (1–6). The nature and morphology of solid surface also play an important role and were more recently investigated using fractal geometry (7–9).

In a previous study (10), we have shown that two commercially available qualities of orthoboric acid (chosen as a model compound), “powder” and “crystal,” in spite of their different names are related to the same crystal network (triclinic). However, particle size distribution appears different from sieving data.

In order to study the effect of particle size on the aqueous dissolution rate, we aimed at:

- Separation of seven particle size classes from bulk powders using sieving
- Study of the particle size distribution of the two bulk powders using laser light scattering
- Evaluation of the dissolution rate of the two bulk qualities
- Study of the dissolution rate of particle size fractions

## MATERIALS AND METHODS

### Materials

Two commercially available qualities of orthoboric acid (AB) were used: “orthoboric acid crystal”, ABC (lot K18999560344, Merck) and “orthoboric acid powder,” ABP (lot 334K19985662, Merck). Measurements are carried out on bulk powders and also on narrowly distributed particle size fractions.

### Methods

#### Particle Size Analysis (11)

**Microscopic observations** Particles were observed with an optic microscope (AXIOPHOT ZEISS) and photomicrographed at suitable magnification.

**Sieving** From 100 g of each bulk powder (ABC or ABP), the particles were separated in particle size fractions using a RETSCH KS1 (250 tr/min; 10 min) or a TAMISOR (frequency 60; 10 min) to give eight fractions: less than 90  $\mu\text{m}$ , 90–125  $\mu\text{m}$ , 125–180  $\mu\text{m}$ , 180–250  $\mu\text{m}$ , 250–355  $\mu\text{m}$ , 355–500  $\mu\text{m}$ , 500–710  $\mu\text{m}$ , and 710–1250  $\mu\text{m}$ . For the two qualities, tests are made in triplicate.

**Laser light scattering** Light scattering according the particles in air (PIA) method, on the bulk qualities using a particle size diffractometer COULTER LS 130, equipped with dry powder module. The particles are suspended in the air during measurement in order to prevent any change that can be due to beginning of dissolution.

For particle sizes larger than the wavelength of the light, a diffraction pattern is observed in the forward direction. The diffraction angle of a monochromatic light beam is a function of the particle size. The detector provided an electronic output signal and the intensity is linked to the number of particle of this size. A deconvolution of the intensity profile provides the result as a volume distribution. Data treatment is based on a Fraunhofer diffraction model, supposing that particles are homogeneous spheres and require no assumption of their optical properties.

Run length is 30 sec; measures are repeated three times. Assuming that particles have a spherical shape, results of the size measurement are given as differential volume distribution.

### Dissolution Testing

Dissolution tests were carried out in a flow-through cell (Dissotest CE1, SOTAX) of an internal diameter of 12 mm (12). During testing, the dissolution medium (bidistilled water) was circulated by pumping (pump CY1D, SOTAX) through cell at fixed flow rate of 15  $\text{cm}^3/\text{min}$  (12). The aqueous dissolution medium was maintained at  $30 \pm 0.5^\circ\text{C}$  using a water-bath (Julabo SW20C). Times of sampling are 15 sec, 30 sec, 45 sec, 1 min, 1 min 30 sec, 2 min, 2 min 30 sec, 3 min, 3 min 30 sec, 4 min, every minute up to 10 min, then every other minute up to the end.

Results are means of four essays and are provided as dissolution profiles:  $dQ/dt$  (millimole/minute) versus  $t$  (minute) (13).

The concentration of each sample was determined using quantitative dosage adapted from the *European Pharmacopoeia* procedure (14), namely, 2  $\text{cm}^3$  aliquots

of each sample were complexed by addition of 10 cm<sup>3</sup> of 0.5 M mannitol and then titrated by aqueous sodium hydroxide (0.1 M).

## RESULTS AND DISCUSSION

### Particle Size Distribution

#### ABC ("Crystal") Quality

**Sieving and microscopic observations** Particle size fractions of ABC quality can easily be classified using a "plane" sieve (RETSCH). The histogram of the particle size distribution obtained by sieving is shown in Fig. 1. The mode of particle size distribution belongs to the 180–250  $\mu\text{m}$ , range.

Microscopic observation shows an equant shape (15) for particles and confirms size homogeneity of sieved particle fractions, as displayed in Fig. 2 for the 90–125  $\mu\text{m}$  particle fraction as an example.

**Laser diffraction (PIA)** Sieve analysis has frequently been used for determining particle size distribution, but in addition to this method, laser diffraction measurement in air provides a rapid and reproducible size distribution determination (16).

The histograms of differential particle size volume distribution for ABC ("crystal") quality, estimated from light scattering are shown in Fig. 3. The particle mean and median diameters found are equal to 272  $\mu\text{m}$  and 297  $\mu\text{m}$ , respectively.

The histogram of particle size distribution obtained by diffraction included 85 classes, whereas sieving gave only 8 classes using present conditions. In order to compare the histograms, it was necessary to group several classes obtained by diffraction to fit those of sieving (17). Assuming that particles have a uniform density

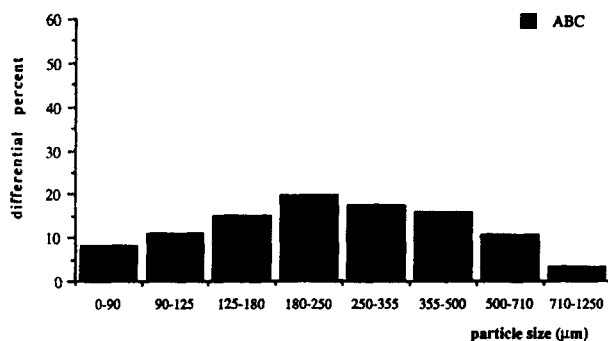


**Figure 1.** Particle size distribution of ABC bulk powder: differential percent from sieving.

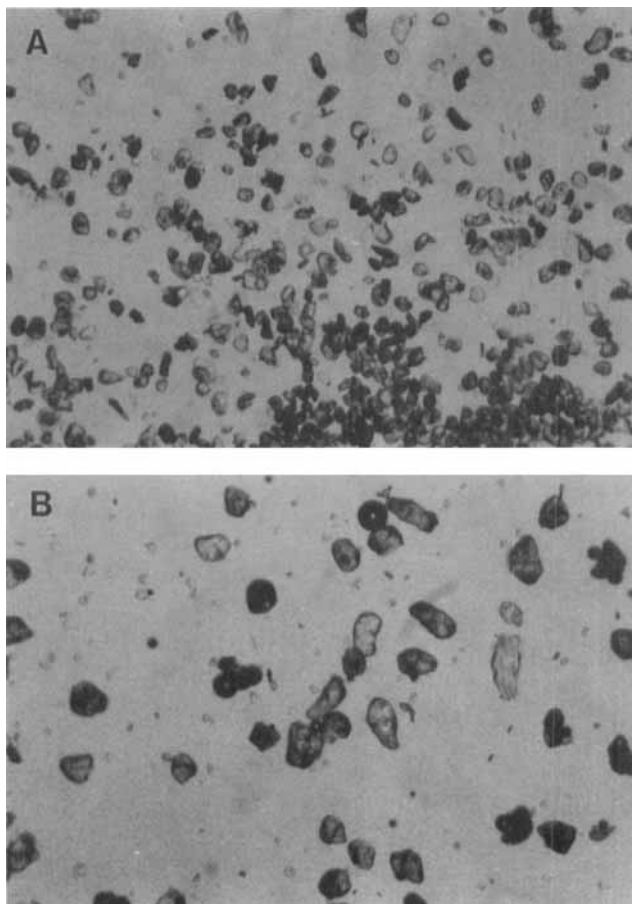


**Figure 2.** Photomicrographs ( $\times 2.5$ ) of 90–125  $\mu\text{m}$  (A) and 180–250  $\mu\text{m}$  (B) particle fractions of ABC.

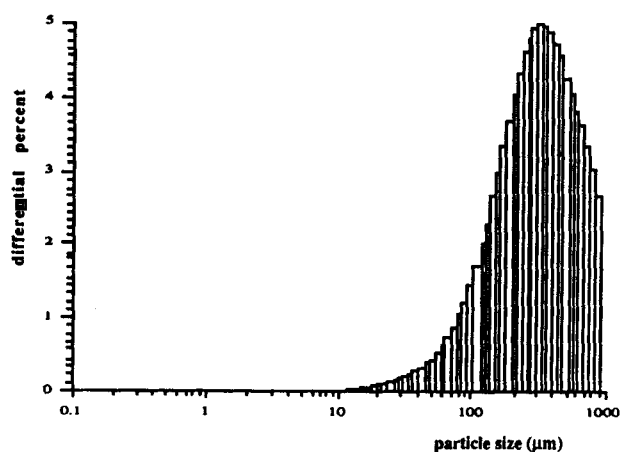


**Figure 3.** Particle distribution of ABC powder measured by laser light scattering.

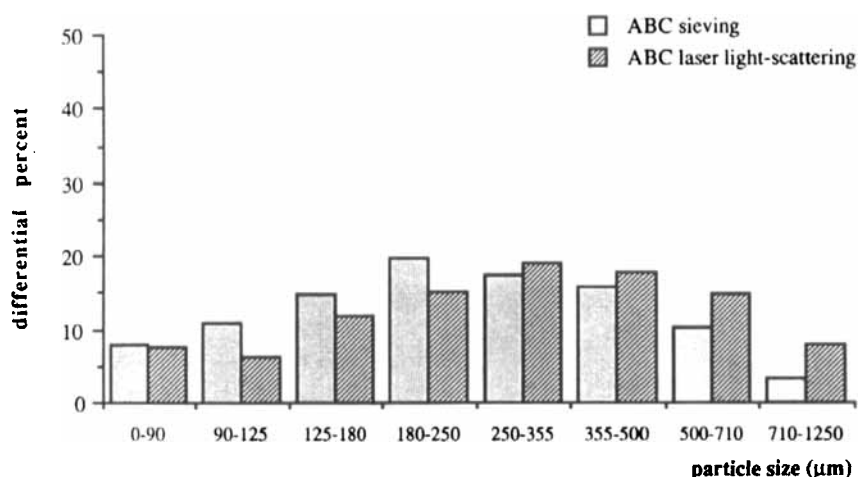


**Figure 4.** Particle size distribution of ABC bulk powder: differential percent from sieving and from laser light scattering.

over the whole distribution, differential percent in weight may also be plotted in the same manner and on the same axis as the differential percentage in volume (Fig. 4).

From sieving data, the mode of particles size distribution belongs to the 180–250 μm size class. On the basis of laser light scattering (Fig. 3), the mode of particles size distribution belongs to 250–355 μm. These two classes, 180–250 μm and 250–355 μm, show the same differential percent (20%) from sieving and from diffraction, respectively.

The shift between the results provided by the two methods, sieving and laser diffraction, seems to be related to the particle shape factor (17,18). It is well established that particle shape causes different dimensional response characteristics in various particle size measuring instruments.

The Fraunhofer model for PIA requires no assumptions of the particles' optical properties but supposes that the particles are homogeneous spheres. In fact, the particle shape differs from spherical form. In this case, it is well known that the difference between the sieve and light diffraction diameter becomes more accentuated.

For elongated shapes the accepted interpretation is that the sieve diameter value is higher than that of the laser diameter, whereas coarse particle with an angular shape give a laser diameter value higher than the sieve diameter (17). In this way, the cumulative profiles obtained by laser light scattering and by sieving are in agreement, as shown in Fig. 5.

#### ABP ("Powder") Quality

**Sieving and microscopic observations** The powder of the ABP quality does not flow easily and fine particles aggregate and also adhere to the sieve (11). For this reason, it was necessary to utilize another sieving method. We tried to use a vibrator sieve shaker

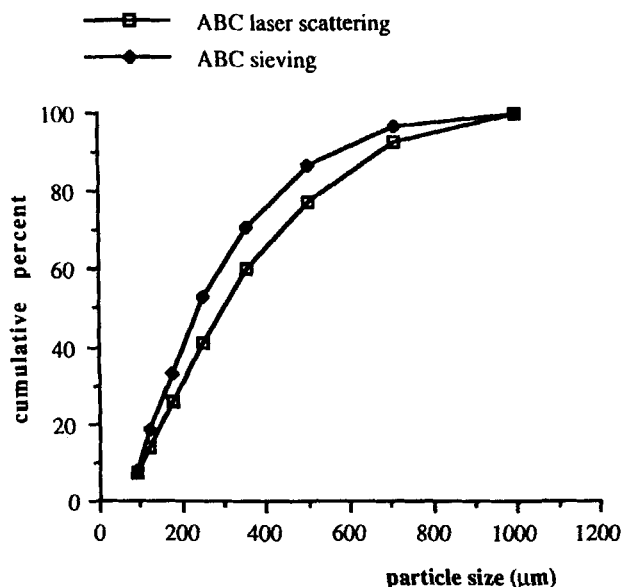


**Figure 5.** Particle size distribution of ABC bulk powder: cumulative percent from sieving and from laser light scattering.



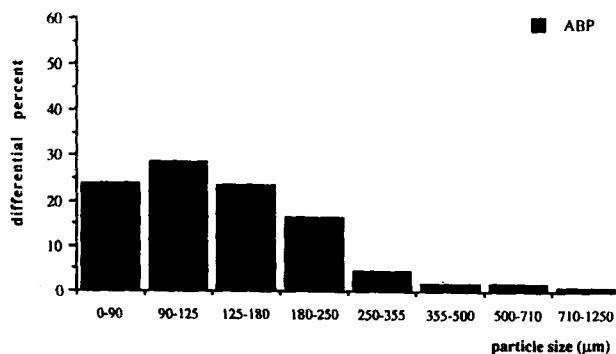


**Figure 6.** Particle size distribution of AB bulk powder: differential percent from sieving.

(TAMISOR). Another histogram of particle size distribution is provided in Fig. 6. From these data, the mode of particle size distribution belongs to the 90–125  $\mu\text{m}$  size class.

Even using TAMISOR, separation of various particle size fractions is unsatisfactory, as pointed out on photomicrographs of recovered fractions on the 90  $\mu\text{m}$  and 180  $\mu\text{m}$  sieve, respectively (Fig. 7). These fractions contain many different size particles, especially small particles.

To provide homogeneous size particle samples, 180–250  $\mu\text{m}$ , 125–180  $\mu\text{m}$  and 90–125  $\mu\text{m}$  particles fractions have been separated by further sieving, from only 20 g of corresponding inhomogeneous fraction and using TAMISOR and the same procedure as previously. We investigated the time dependence of the sieving process, and found that after 15 min of sieving, percentage of weight passed through the sieve did not exceed 15% of initial weight. This preparative procedure provided a homogeneous particle size fraction, as shown in Fig. 8 for 90–125  $\mu\text{m}$  particles powder, chosen as an example.

**Laser diffraction** From laser diffraction data, ABP powder is widely constituted by particles smaller than 90  $\mu\text{m}$  (mean and median of distribution are equal to 65  $\mu\text{m}$  and 86  $\mu\text{m}$ , respectively) and contains no particle size larger to 500  $\mu\text{m}$  as shown in Fig. 9.

With the aim of comparing the histograms of particle size distribution obtained by diffraction and by sieving, particle size classes obtained by diffraction are grouped in order to fit those of sieving, as previously described for ABC quality (Fig. 10).

The histogram of differential particle size distribution provided by this sieving procedure shows no close re-

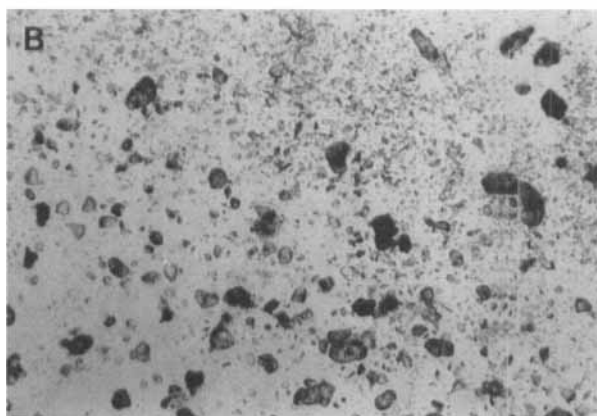
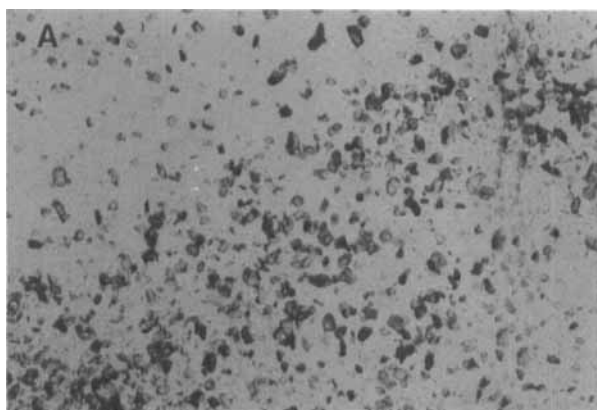


**Figure 7.** Photomicrographs ( $\times 2.5$ ) of ABP powders collected from 90  $\mu\text{m}$  (A) and 180  $\mu\text{m}$  (B) sieves.

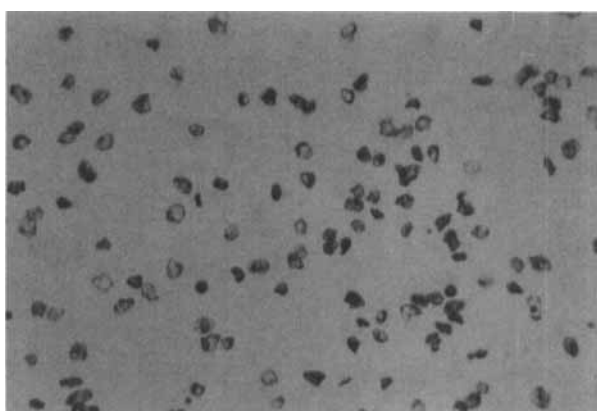


**Figure 8.** Photomicrograph ( $\times 2.5$ ) of further sieved 90–125  $\mu\text{m}$  particles from ABP.

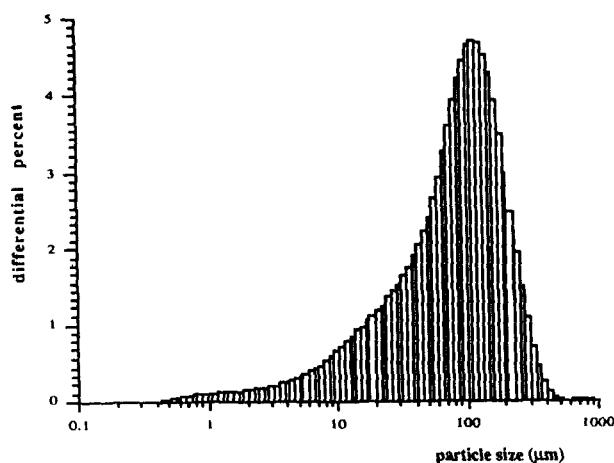


**Figure 9.** Particle distribution of ABP powder measured by laser light scattering.

semblance to the differential particle size profile from laser light scattering (Fig. 10). Furthermore, cumulative profiles are also different, as shown in Fig. 11. In particular, the particles of  $<90\ \mu\text{m}$  constitute more than 50% of the whole quantity of powder as shown by laser diffraction data, instead of only 24% of this powder as it appears from sieving data.

This discrepancy can be pointed out on the basis of microscopic data, as reported in Fig. 7, which shows the presence of fine particles ( $<90\ \mu\text{m}$ ) in the 90–125  $\mu\text{m}$  and 180–250  $\mu\text{m}$  fractions, chosen as examples. So,

weight percent of the smallest particles is not taken in account in sieving result.

### Dissolution Testing

To carry out dissolution rate studies, we chose a continuous flow-through cell dissolution apparatus in an open system. This dissolution method, the flow-through cell approach, has received some attention in recent years (12,19,20). Some investigators demonstrated that a good correlation could be established between in vitro drug release and in vivo drug absorption (21,22). Many advantages of flow-through system have been outlined (19):

- Maintains sink conditions in a theoretically perfect state
- Has built-in filtration
- Provides mathematically definable flow patterns because of an ideal hydrodynamic homogeneous system
- Produces data in a differential form, so that the dissolution profile indicates the concentration (millimoles/minutes) being dissolved at any given instant

### Dissolution Testing on Bulk Qualities

These two qualities, ABC and ABP, which have very different particle size distributions have different dissolution profiles as shown in Fig. 12.

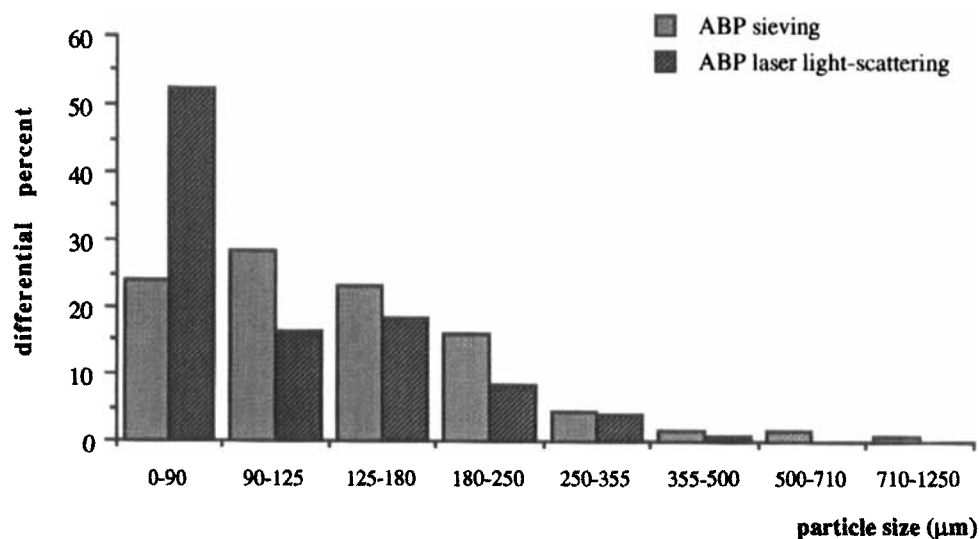


**Figure 10.** Particle size distribution of ABP bulk powder: differential percent from laser light scattering and from sieving.

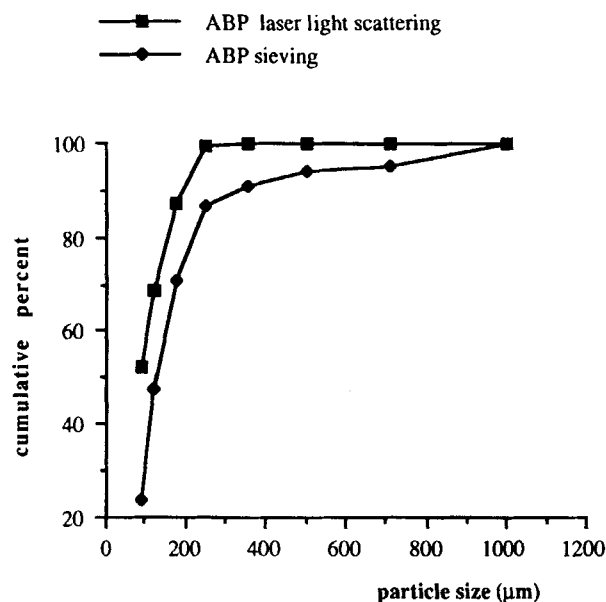


**Figure 11.** Particle size distribution of ABP bulk powder: cumulative percent from laser light scattering and from sieving.

For ABC quality, this graph shows a maximum at less than 1 min and tends towards zero within 10 min, corresponding with the total sample dissolution.

For ABP quality we cannot observe a maximum, but we notice a flattened-out curve within the first 3 min of dissolution. We can see that this graph tends towards zero within 20 min, which means twice the time for complete dissolution.

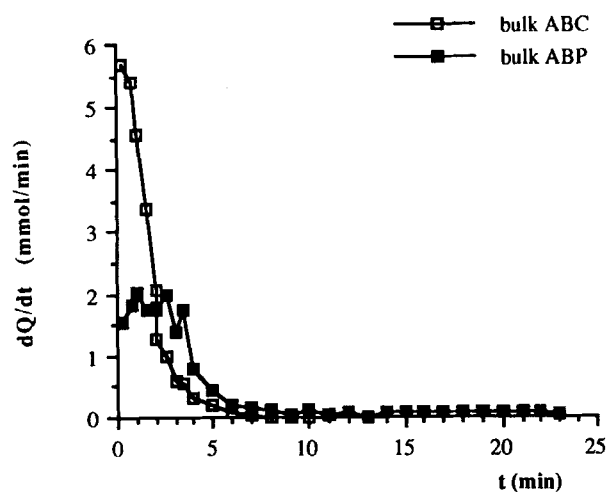


**Figure 12.** Dissolution rate of ABC and ABP bulk powders.

This slower dissolution can be related: (i) to the particle size distribution, (ii) to a different shape for the same size of each of two qualities, (iii) to these two causes simultaneously.

Attempting to achieve a better understanding of these different dissolution profiles, we attempted to separate many narrowly distributed particle size fraction from the two bulk qualities and, therefore, to study their dissolution rates.

#### Dissolution Testing on Homogeneous Particle Size Fractions

For dissolution studies, four different particle size samples for each quality, ABC and ABP, were used, namely less than 90  $\mu\text{m}$ , 90–125  $\mu\text{m}$ , 125–180  $\mu\text{m}$ , 180–250  $\mu\text{m}$ ; and for ABC quality, more, the three fractions 250–355  $\mu\text{m}$ , 355–500  $\mu\text{m}$ , and 500–710  $\mu\text{m}$ . Indeed, for the classes above 250  $\mu\text{m}$  size, ABP quality allowed only a small percentage in weight (<5%) and for this reason was not investigated.

For ABC quality, the three fractions 250–355  $\mu\text{m}$ , 355–500  $\mu\text{m}$ , and 500–710  $\mu\text{m}$  display neighboring dissolution profiles, as displayed in Fig. 13. Profiles of these fractions are similar to dissolution profile of bulk ABC (Fig. 12). In particular, both profiles show a maximum of dissolution rate, above 3.5 mmol/min, at the first time of dissolution.

As displayed in Figs. 14 and 15, the four fractions, 125–180  $\mu\text{m}$  and 180–250  $\mu\text{m}$  particles from ABC and from ABP, have very close dissolution profiles.

In the same way, dissolution profiles of 125–180  $\mu\text{m}$  and 180–250  $\mu\text{m}$  (Figs. 14 and 15) are close to the dis-

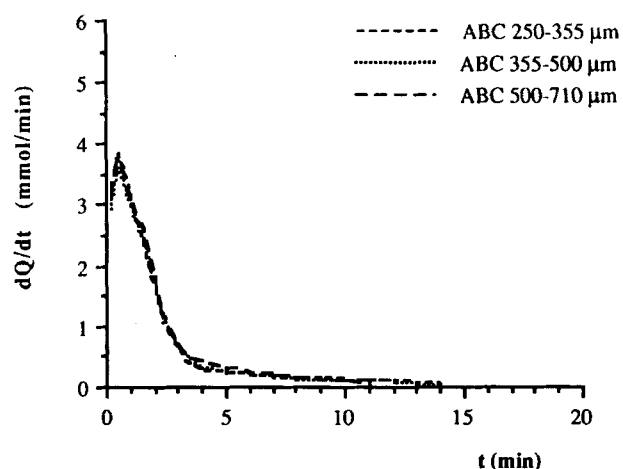


**Figure 13.** Dissolution rate of 250–355, 355–500, and 500–710  $\mu\text{m}$  particle samples from ABC.

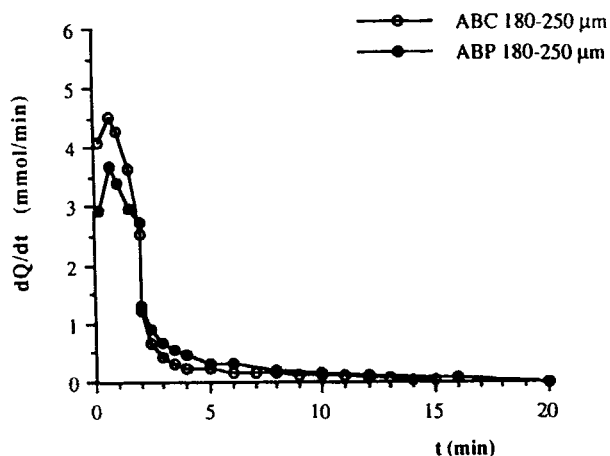


**Figure 14.** Dissolution rate of 180–250  $\mu\text{m}$  particle sample from ABC and from ABP.

solution profiles of 250–355  $\mu\text{m}$ , 355–500  $\mu\text{m}$ , and 500–710  $\mu\text{m}$  (Fig. 13) of ABC quality (Fig. 12).

As shown in Fig. 16, the dissolution profile of 90–125  $\mu\text{m}$  particles from ABC powder show even close resemblance to dissolution profiles previously described (Figs. 13–15), but dissolution behavior are revealed to be different from 90–125  $\mu\text{m}$  particles of ABP powder (Fig. 16). Indeed, starting from a weak maximum value (below 2 mmol/min), the dissolution rate decreases at the very beginning of dissolution. Thereby, while the dissolution of 90–125  $\mu\text{m}$  particles from ABC is nearly complete at the end of 15 min, more time is necessary

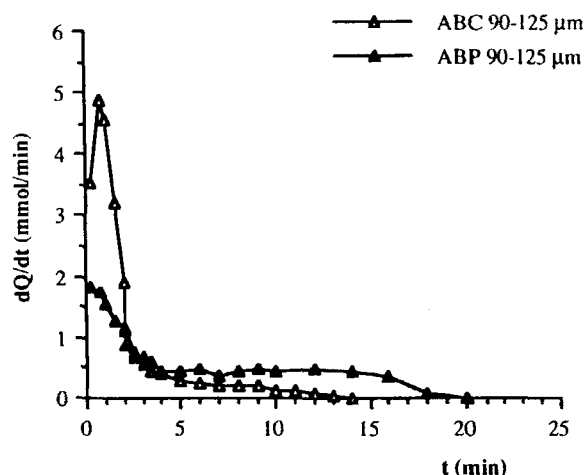


**Figure 16.** Dissolution rate of 90–125  $\mu\text{m}$  particles from ABC and from ABP.

to perform complete dissolution of 90–125  $\mu\text{m}$  particles from ABP.

In order to determine the role played by the sieve operating conditions, 90–125  $\mu\text{m}$  particles of ABC powder were subjected to sieving on the TAMISOR. The TAMISOR-sieved 90–125  $\mu\text{m}$  fraction was also tested. As shown in Fig. 17, the two 90–125  $\mu\text{m}$  particle powders separated on TAMISOR have similar dissolution profiles; in other words, the sieving process have an effect upon dissolution behavior of 90–125  $\mu\text{m}$  particles.

This result cannot be explained by breaking of particles. Based on microscope observations, no difference

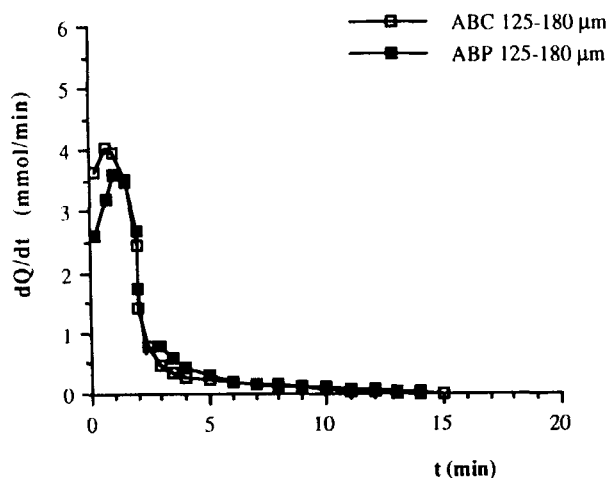


**Figure 15.** Dissolution rate of 125–180  $\mu\text{m}$  particle sample from ABC and from ABP.

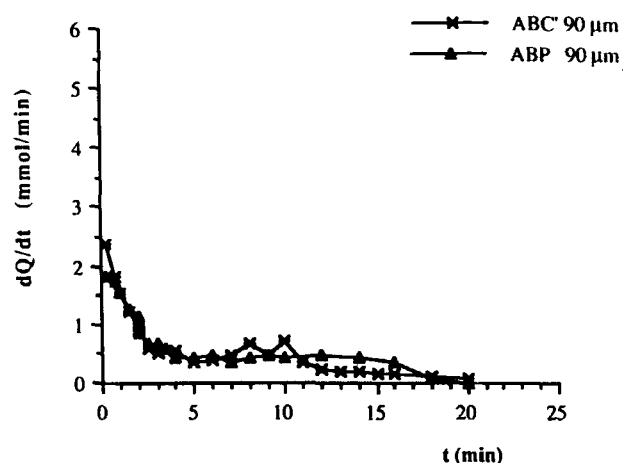


**Figure 17.** Dissolution rate of 90–125  $\mu\text{m}$  particles from ABC and from ABP separated on TAMISOR.



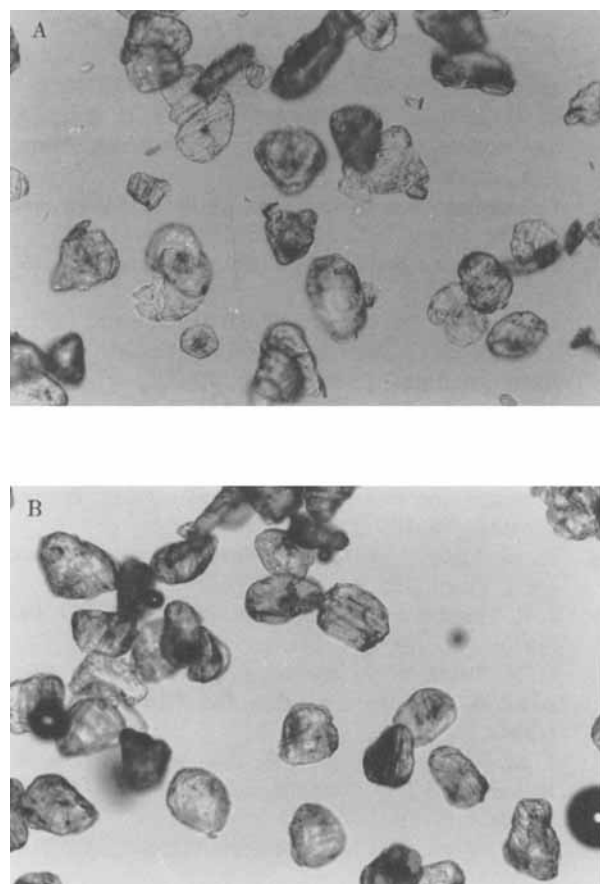


**Figure 18.** Photomicrographs ( $\times 10$ ) of 90–125  $\mu\text{m}$  particle sample of ABC after RETSCH sieving (A) and from ABC after TAMISOR sieving (B).

appears in particle morphology between the two 90–125  $\mu\text{m}$  particle samples (Fig. 18).

The time of dissolution of 0–90  $\mu\text{m}$  particles is about 20 min for ABC and 40 min for ABP. The rate of dissolution remains weak throughout dissolution, close to 1 mmol/min at the beginning, and then decreases (Fig. 19). For that very reason, it shows resemblance to the dissolution of the bulk ABP powder. We can infer that presence of fine particles slackens the rate of dissolution.

### CONCLUSION

For “crystal” ABC and “powder” ABP, the dissolution rate appears very different. The ABC quality dissolves more rapidly than the ABP quality particle size.

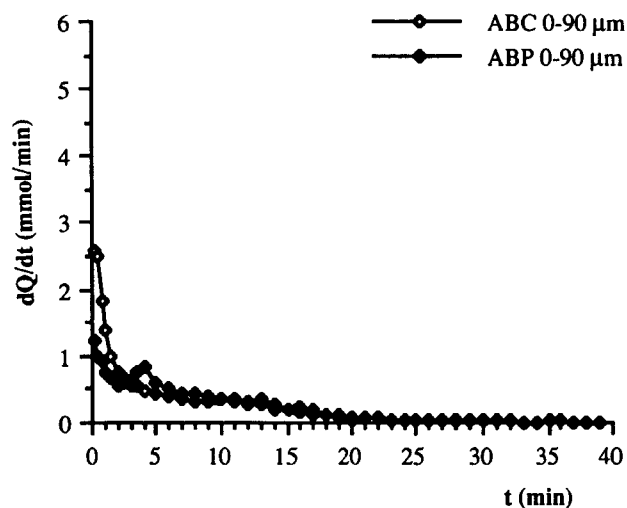


**Figure 19.** Dissolution rate of 0–90  $\mu\text{m}$  particle sample from ABC and from ABP.

On the basis of sieving and laser light-scattering results, the range of the granulometric distribution is from 0–90  $\mu\text{m}$  to 500–710  $\mu\text{m}$  for the ABC quality (mean and median diameters equal to 272  $\mu\text{m}$  and 297  $\mu\text{m}$ , respectively). ABP quality contains no particles larger than 500  $\mu\text{m}$ , and half the weight of the powder is constituted by particles less than 90  $\mu\text{m}$ .

Laser light-scattering data are in good agreement with sieving results for ABC quality, taking into account the fact that laser diameter values are higher than the sieve diameter value. With regard to ABP quality, differential particle size distribution provided from the sieving technique show no close resemblance to the differential particle size profile from laser diffraction. But, separation of ABP size is difficult because powder particles aggregate and adhere to the sieve. For this reason, laser light-scattering appears to be a more reliable method for measuring size distribution of ABP quality.

It is generally expected that fine powders have a faster dissolution rate. However, in our case, the ABP quality with a high fine particle content has the lower rate of dissolution. Our dissolution results clearly show that the mean particle size of orthoboric acid plays an important role in the dissolution rate. The slower dissolution rate can be tentatively assigned to the presence of < 90  $\mu\text{m}$  particles, in spite of maximum resulting surface area (23). It appears that sieve conditions influence dissolution behavior of 90–125  $\mu\text{m}$  particles.

With the aim of explaining the influence of the particle size on dissolution behavior of these two orthoboric

acid qualities, further works are in progress to investigate wettability and surface characteristics.

### ACKNOWLEDGMENTS

Thanks are due to Dr. J. Bonvalot (Université de Bourgogne, Laboratoire des Sciences de la Terre) and to Dr. P. Bracconi (Université de Bourgogne, Laboratoire de Réactivité des Solides) for providing laboratory facilities. We gratefully thank J.-C. Gnanou for his work on dissolution studies.

### REFERENCES

1. N. Kaneniwa and N. Watari, *Chem. Pharm. Bull.*, **22**, 1699 (1974).
2. J. T. Carstensen and M. N. Musa, *J. Pharm. Sci.*, **61**, 223 (1972).
3. R. J. Hintz and K. C. Johnson, *Int. J. Pharm.*, **51**, 9 (1989).
4. P. J. Meyer, N. Khoury, S. A. Howard, and J. W. Mauger, *Drug Dev. Ind. Pharm.*, **18**, 395 (1992).
5. N. O. Lindberg and T. Lundstedt, *Drug Dev. Ind. Pharm.*, **20**, 2547 (1994).
6. N. Kitamori and K. Iga, *J. Pharm. Sci.*, **67**, 1674 (1978).
7. D. Farin and D. Avnir, *J. Pharm. Sci.*, **81**, 54 (1992).
8. M. J. Fernandez-Hervas, M. A. Holgado, A. M. Rabasco, and A. Fini, *Int. J. Pharm.*, **108**, 187 (1994).
9. Y. J. Sun, B. Tang, and N. Y. Chen, *Chin. Sci. Bull.*, **38**, 1310 (1994).
10. C. Andrès, A. Ndiaye, A. Tromelin, B. Chaillot, and Y. Pourcelot, *Drug Dev. Ind. Pharm.*, **21**, 1875 (1995).
11. H. G. Brittain, S. J. Bogdanowich, D. E. Buay, J. DeVincentis, G. Lewen, and A. W. Newman, *Pharm. Res.*, **8**, 963 (1991).
12. F. Langenbücher, D. Benz, W. Kürth, H. Möller, and M. Otz, *Pharm. Ind.*, **51**, 1276 (1989).
13. J. E. Tingstad and S. Riegelman, *J. Pharm. Sci.*, **59**, 692 (1970).
14. *Pharmacopée Européenne*, 10<sup>e</sup> ed, Misonneuve, 1985.
15. T. A. Barber, *Pharmaceutical Particulate Matter*, Interpharm Press, Buffalo Grove, 1993.
16. C. Washington, *Particle Size Analysis in Pharmaceutical and Other Industries*, E. Howard, New York, 1992.
17. N. Nathier-Dufour, L. Bourgeard, M. F. Devaux, D. Bertrand, and F. Le Deshault de Monderon, *Powder Technol.*, **76**, 191 (1993).
18. A. M. Juppo, J. Ylirussi, L. Kervinen, and P. Ström, *Int. J. Pharm.*, **88**, 141 (1992).
19. J. E. Tingstad and S. Riegelman, *Pharm. Sci.*, **59**, 692 (1970).
20. G. H. Zhang, W. A. Vadino, T. T. Yang, W. P. Cho, and I. A. Chaudry, *Drug Dev. Ind. Pharm.*, **20**, 2063 (1994).
21. J. M. Aiache, M. Islasse, E. Beyssac, S. Aiache, R. Renoux, and J. P. Kantelip, *Int. J. Pharm.*, **39**, 235 (1987).
22. J. G. Philips, Y. Chen, and I. N. Wakeling, **15**, 2177 (1989).
23. A. Noyes and W. Whitney, *Z. Phys. Chem.*, **23**, 689 (1897).